E-proceedings of the 36th IAHR World Congress
28 June – 3 July, 2015, The Hague, the Netherlands

FLUID MECHANICS, SEDIMENT TRANSPORT AND MIXING ABOUT THE CONFLUENCE OF NEGRO AND SOLIMÕES RIVERS, MANAUS, BRAZIL

MARK TREVETHAN[(1)], ANDRE MARTINELLI[(2)], MARCO OLIVEIRA[(2)], MARCO IANNIRUBERTO[(3)] & CARLO GUALTIERI[(1)]

[(1)] *Department of Civil, Construction and Environmental Engineering, University of Napoli Federico II, Napoli, Italy, mark.trevethan@gmail.com; carlo.gualtieri@unina.it*

[(2)] *Geological Survey of Brasil (CPRM), Manaus, Brazil, andre.santos@cprm.gov.br; marco.oliveira@cprm.gov.br*

[(3)] *Institute of Geosciences, University of Brasilia, Brasilia, Brazil, ianniruberto@unb.br*

ABSTRACT

As part of a project to investigate the hydrodynamic, sediment transport and mixing processes about the large confluences of the Amazon River, a field study was conducted about the confluence of the Negro and Solimões Rivers. This confluence ranks among the largest confluences on Earth the outcomes of this study may also provide some general insights into large confluence dynamics. A detailed series of ADCP, water quality and seismic profile measurements were collected to investigate key hydrodynamic and morphodynamic features about this confluence. Presented here are the key hydrodynamic features observed about this large confluence and how these relate to findings in previous studies conducted in flumes and small confluences. Finally some insights into how the differences in water characteristics and the hydrodynamics of these two rivers may influence the rate of mixing downstream are presented.

Keywords: Amazon River; Confluence; Hydrodynamics; Mixing; Sediment transport

1. INTRODUCTION

In the last decades a wide body of theoretical, numerical, experimental and field research has emerged on the fluvial dynamics of river confluences. To date most experimental studies have focused either on laboratory confluences (e.g. Best, 1987) or on small natural confluences (e.g. Kentworthy and Rhoads, 1995), whereas an extremely limited number of investigations conducted on large river confluences, i.e. channel widths > 100 m (e.g. Lane et al., 2008; Konsoer and Rhoads, 2014). Further, to date numerical studies have generally only focused on simulating the flow structure observed in laboratory (e.g. Huang et al., 2002) and small natural confluences (e.g. Constantinescu et al., 2011).

As the flows from two tributaries merge and adjust to the confluences planform geometry substantial changes to the flow hydrodynamics and bed morphology occur within and immediately downstream of the confluence (Mosley, 1976). This region where the local hydrodynamics are influenced by the convergence and realignment of the combining flows at the confluence is known as the Confluence Hydrodynamic Zone (Kentworthy and Rhoads, 1995). It is generally acknowledged that the hydrodynamics and morphodynamics (i.e. patterns of erosion and deposition) within the confluence hydrodynamic zone (CHZ) are influenced by the planform of the confluence; junction angle of confluence (α in Figure 1); momentum flux ratio of merging streams (M_R); and level of concordance between channel beds at the confluence entrance (Mosley, 1976; Best, 1987). Further it is generally acknowledge that any differences in the water characteristics (e.g. temperature, conductivity, suspended sediment concentration) between the incoming tributary flows may also impact on the local processes about the confluence (e.g. Rhoads and Kentworthy, 1998; Biron and Lane, 2008).

The fluid dynamics about confluences have a highly complex three-dimensional flow structure which generally includes a zone of flow stagnation near upstream junction corner; an area of flow deflection as tributary flows enter confluence; shear layer and/or mixing interface between the two converging flows; a possible zone of separated flow about the downstream junction corner(s); flow acceleration within the downstream channel; and flow recovery at the downstream end of the CHZ as illustrated in Figure 1 (Best, 1987). Depending on the angles between the two incoming rivers with the downstream channel, and the momentum flux ratio between the confluents, the mixing interface may display Kelvin-Helmholtz or wake mode type flow characteristics (e.g. Rhoads and Sukhodolov, 2008). Helical flow cells are also often observed about confluences, however, the presence and characteristics of these helical cells at confluences remains controversial within the scientific community (e.g. Constantinescu et al., 2011).

The confluence bed morphology can generally be related to the different hydrodynamics zones found about confluences (e.g. Best, 1987; 1988). Common morphological features often observed about confluences include: a scour hole normally orientated along the region of maximum velocity where both flows begin to converge; avalanche faces at mouth of each tributary; sediment deposition within the stagnation zone; and bars formed within possible flow separation zones or mid-stream in downstream channel (e.g. Szupiany et al., 2009). Another morphological feature observed at a high portion of confluences is a bed discordance (i.e. one tributary bed is higher than the other), which can be formed through differences in channel discharges and bed geology (e.g. Gaudet and Roy, 1995). More generally, the patterns of erosion and deposition within the CHZ reflect the spatial variations in bed shear stress (Rhoads et al., 2009). Ultimately, the bed shear stress and sediment transport can be related to the localised fluctuations in flow velocity (e.g. turbulence) generated through the interaction of the flow with both vertical and horizontal variations in channel bathymetry causing the flow accelerate or decelerate (e.g. Best and Rhoads, 2008).

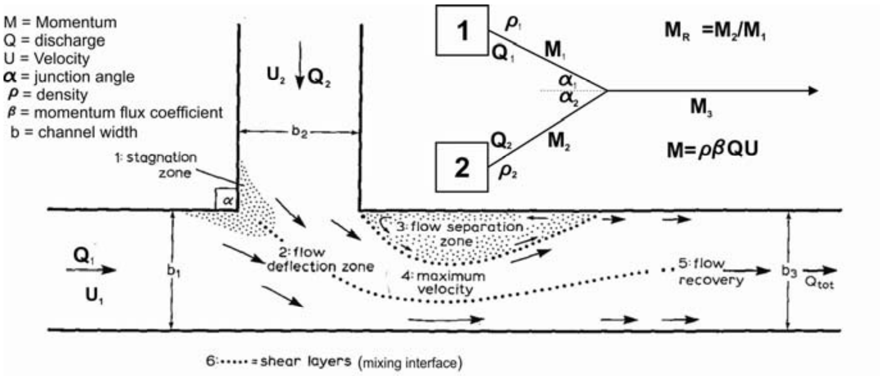

Figure 1. Descriptive model of flow dynamics and key hydrodynamic features about a confluence, slightly modified from Best (1987).

A fundamental feature of natural confluences is the development of a mixing interface between the converging flows due to contrasts in the water characteristics (e.g. temperature, suspended sediment concentration) of the two tributaries (e.g. Rhoads and Sukholodov, 2008). Previous studies such as Rhoads and Kentworthy (1998) and Ramon et al. (2013) have observed that these contrasts in water characteristics may form a lateral stratification layer between the confluent flows which limits the amount mixing within the CHZ. Thereby under the right conditions mixing interfaces have been observed large distances downstream in natural confluences (e.g. MacKay, 1970). Conversely, studies such as Gaudet and Roy (1995) have shown that under certain conditions the interaction of the hydrodynamics and bathymetry about the confluence may greatly enhance the mixing of the confluent flows.

Presently little is understood about how river confluence hydrodynamics may vary with river size, especially in the largest rivers (e.g. Parsons et al., 2008). Many field observations about large river confluence indicate that mixing of the confluent flows may take 10's to 100's of kilometres to complete (e.g. MacKay, 1970). However, Lane et al. (2008) found that under exactly the right flow conditions for the confluence bathymetry rapid mixing may occur downstream of a large river confluence, and suggested that these different confluence mixing rates are dependent upon basin-scale hydrological responses, which are likely to differ significantly between large and small confluent rivers. More recently, Ramon et al. (2013) showed that seasonal variability between the tributary sources caused water characteristic differences in the confluent flows that may effect the type and level of stratification occurring at the junction and in turn the level of mixing downstream of the confluence. In a different large confluence study, Parsons et al. (2007) indicated that large-scale bed-roughness (e.g. dunes) often observed in large rivers may dominate the flow and lead to the absence of channel-scale helical flow cells observed about smaller confluences. Finally, Barua and Rahman (1998) observed in a large river horizontal turbulent motion with periods between 18 and 30 minutes which indicated possible horizontal turbulence structures scaling with the channel width. These initial field studies in large river confluences highlight some significant differences between the dynamics of large and small confluences that require further investigation. Presented here are some initial results from a field campaign conducted about the confluence of the Negro and Solimões Rivers, which is one of the largest confluences on Earth. These initial results are primarily focused on the observed hydrodynamics about this large confluence during this field study and provide some interesting insights into the confluence hydrodynamics and how these relate to the local mixing and sediment transport processes.

1.1 Field site and Instrumentation

The confluence of the Negro and Solimões Rivers is located near Manaus in Northern Brazil, where these rivers merge to form the Amazon River approximately 1,600 km upstream from it's mouth at the Atlantic Ocean. This confluence is famous for the meeting of the black (Negro) and white (Solimões) waters of the two rivers (called locally "Encontro das Aguas"), which may be visually observed not mixing for over 100 km downstream. The distinct waters of these two rivers are related to the locations of the two catchments within the Amazon Basin, with the Negro catchment (area = 687,000 km^2) located in the North draining the Western slopes of the Guyana Shield, while the Solimões catchment (area =

2,150,000 km^2) is located in the West of the basin with it's sediment rich waters originating from the Andes (e.g. Laraque et al., 2009). There is also a relatively large difference in the volumetric discharge from the Negro and Solimões Rivers with average discharges of approximately 27,000 and 103,000 m^3/s respectively.

As part of the CLIM-Amazon Project (a joint European and Brazilian project studying climate and sedimentary processes of the Amazon River Basin) an investigation was conducted about the confluence of the Negro and Solimões Rivers to help understand the fluid dynamics, sediment transport and mixing about the large confluences of Amazon River. Within this investigation a field study (CNS1) was conducted during "low flow conditions" for Solimões River in October 2014 about the confluence hydrodynamic zone (CHZ). During this field study a detailed series of ADCP and seismic transects, as well as water quality measurements were collected to investigate key hydrodynamic and morphodynamic features about this confluence (e.g. Figure 2). Figure 2 provides a map of the confluence for the Negro and Solimões Rivers indicating all sampling locations about the confluence hydrodynamic zone collected during the field study.

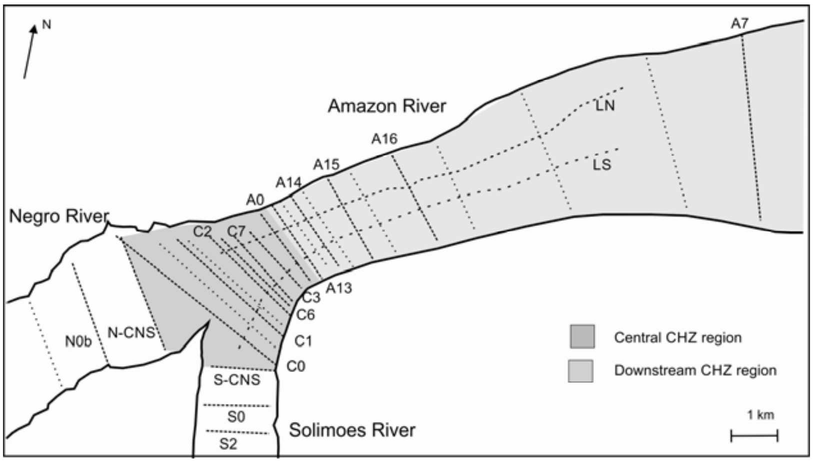

Figure 2. Map of confluence for Negro and Solimões Rivers, with sampling positions from during Field Study CNS1 highlighted.

During the Field Study CNS1, a Teledyne RDI 600 kHz Rio Grande acoustic Doppler current profiler (ADCP) was used to collect cross-sectional measurements at key locations about the confluence, as indicated by dotted lines in Figure 2. The ADCP was used to measure three-dimensional water velocities over the water depth along the transect, as well as water temperature near the surface and backscatter intensity which is related to suspended sediment concentration (e.g. Szupiany et al., 2009). Due to the extreme sampling conditions (i.e. flow velocities up to 3 m/s, turbulent eddies larger than 40 m) a constant boat speed of approximately 2 m/s was used while collecting these transects to ensure minimal lateral variations about the transect line. These ADCP transects shown in Figure 2 were collected over 5 days (28/10-1/11/2014) with multiple transects collected at many of 27 the locations about the CHZ. The transects discussed herein are highlighted in bold and labelled in Figure 2. In addition to the cross-sectional measurements, two longitudinal profiles one on each side of the Amazon River were collected as well as water samples at surface, 10 m, and 20 m depths at twelve locations about confluence. These water samples were used to understand the characteristics of the two tributary rivers (e.g. temperature, pH, conductivity) and measure local suspended sediment concentration (SSC) and oxygen isotope values. The range for the suspended sediment concentration/total suspended solids observed was 0.1 > SSC > 0.2 g/L and SSC < 0.01 g/L in the Solimões and Negro waters respectively. These observed SSC values on the Solimões River are similar to those observed by Richey et al. (1986) under similar low flow conditions. The small values observed on the Negro River reflect the amount of suspended organic matter, as the Negro River is not generally known for carrying suspended sediment (e.g. Laraque et al., 2009).

2. KEY OBSERVATIONS

The primary focus herein are the ADCP transects collected during the Field Study CNS1 on 31/10/2014 (Figure 3). Figure 3 shows the depth-averaged velocity data (magnitude and direction) collected at each location about the confluence of the Negro and Solimões Rivers. Table 1 presents the measured median flow properties on 31/10/2014 and water characteristics of the Negro and Solimões Rivers at the ADCP transects just upstream of the confluence. The values presented in Table 1 are typical of the flow properties measured with ADCP and water characteristics observed over the main five days of sampling for the Field Study CNS1. In Table 1, it can be seen that distinct differences in the water characteristics of the two rivers were observed, with these measured differences in water characteristics being similar to those observed in previous studies about the confluence (e.g. Laraque et al., 2009).

Previous confluence studies have largely acknowledged that the momentum flux ($M_R=\rho_2Q_2U_2/\rho_1Q_1U_1$), discharge ($Q_R=Q_2/Q_1$) and velocity ($U_R=U_2/U_1$) ratios can be related to the observed hydrodynamic and morphodynamic features about the confluence, where ρ = water density (kg/m^3); Q = discharge (m^3/s); U = average cross-sectional velocity (m/s); and herein the subscripts 1 and 2 represent the Solimões and Negro Rivers respectively. From Table 1 the observed values of these key ratios on 31/10/2014 are approximately M_R= 0.112; Q_R= 0.379; and U_R= 0.299 respectively. The relatively low values of these ratios are indicative of the large difference in the flow properties of the two tributary rivers. It is worth noting that there is a large junction angle of approximately 80° between the Negro and Solimões Rivers, with the junction angle between the Solimões and Amazon Rivers being approximately 110° (see Figure 2). These large junction angles of the Solimões with the Negro and Amazon Rivers means that the Solimões River effectively enters confluence almost perpendicular to the main flow direction of the Amazon and Negro Rivers, and thereby the waters of the Solimões must undergo a large change in flow direction (60-70°) as it becomes the Amazon River (e.g. Figure 3). At the beginning of the central confluence region the width is approximately 4.9 km about transect C0 and narrows to approximately 2 km about the transects C3 and A0 near the start of the Amazon River, with the channel width gradually expanding to over 5 km about 15 km downstream. In the last 2 km leading up to the confluence the Solimões River has a channel width of approximately 1.7 km, while the channel width of the Negro River expands from approximately 2.5 to 2.9 km.

Table 1. Main flow properties and water characteristics of Negro and Solimões Rivers on 31/10/2014.

	Q (m^3/s)	A (m^2)	U (m/s)	FD (°)	W (m)	H (m)	ρ (kg/m^3)	T (C)	pH	Cond. (mS/cm)	Turb. (NTU)	M (kgm/s^2)
Solimões	63,380	40,174	1.34	350	1700	25.0	995.443	30.1	7.2	81	106	85,717,573
Negro	24,030	67,173	0.4	60	2700	25.2	995.293	30.6	5.4	7	0	9,591,000

Legend: Q = discharge; A = cross-sectional area; U = median cross-sectional velocity magnitude; FD = median flow direction degrees from North; W = width; H = median depth; ρ = water density(based on water temperature); T = water temperature; Cond. = water conductivity; Turb. = turbidity; M = momentum flux.

The 15 ADCP transects collected within a 16 km study region about the Negro/Solimões confluence on 31/10/2014, include: two transects on the Negro River; three transects on the Solimões River; five transects in the central CHZ region of the confluence; and five in the downstream CHZ region on the Amazon River. Figure 3 shows that on the Negro River at both transects N0 and N-CNS the flow velocity is relatively uniform over the channel width, with a median value of 0.4 m/s. Conversely in the Solimões, the depth-averaged velocity distribution varies over the channel width, from approximately 2 m/s in the main channel near the right back and decreases almost linearly towards the left bank, with a depth-averaged velocity of approximately 1 m/s observed at the left side of the three Solimões transects (S2, S0 and S-CNS). As these two rivers enter the confluence, its width is approximately 5 km, with the two waters merging about a strong and easily visible mixing interface. For the low flow conditions observed during this field study, this mixing interface began approximately 100 m upstream on the Solimões side of the central spit between the two rivers, with evidence of a stagnation zone between the two waters either side of the central spit. Further, the upstream extent of the stagnation zone seems to end before the location of transect C0, with two waters being deflected and locally aligned about the mixing interface by this transect.

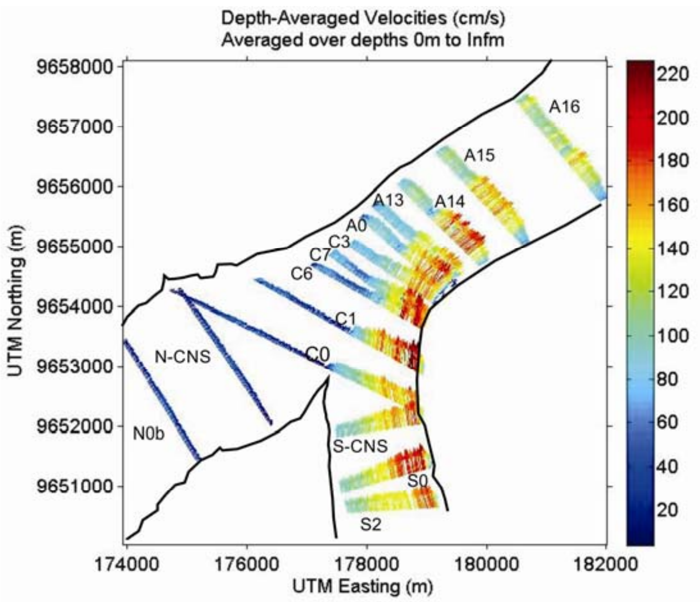

Figure 3. Depth-averaged velocities of ADCP transects collected about confluence of Negro and Solimões Rivers on 31/10/14. Figures were plotted using the Velocity Mapping Tool software (e.g. Parsons et al., 2013).

Table 2 shows the flow properties within the central confluence region and Amazon River on 31/10/2014, presenting the depth-averaged flow velocity magnitude and direction for the Negro, mixing interface and Solimões portions of the confluence and channel, with the median parameter value for each portion listed. Herein the Solimões, Negro and mixing interface portions of each transects were determined herein using the depth-averaged ADCP backscatter intensity (BS) from transects collected on Negro (e.g. N0b) and Solimões (e.g. S0) Rivers on 31/10/2014, with thresholds of BS > 84 dB and BS < 72 dB used for the Solimões and Negro waters respectively. Anything between these two thresholds for unmixed waters of Negro and Solimões Rivers was characterised as being part of the mixing interface. During this field study the extents of the mixing interface was clearly discernable from the pure waters of the Negro ("black") and Solimões ("white") as a blended colour of the two waters.

Table 2. Main flow properties about confluence and Amazon River on 31/10/2014.

	D (m)	W (m)	H (m)	U (m/s)	FD (°)	U_N (m/s)	FD_N (°)	U_{MI} (m/s)	FD_{MI} (°)	U_S (m/s)	FD_S (°)	ΔU (m/s)	$ΔU_{max}$ (m/s)
C0	220	4850	28.5	0.72	103	0.38	61	0.25	119	1.41	281	1.03	1.5
C1	850	3430	34.7	0.53	63	0.45	63	0.42	58	1.49	66	1.04	2.0
C6	1530	2320	43.5	0.9	44	0.55	57	0.56	39	1.59	32	1.04	1.5
C7	1730	2200	44.1	1.34	35	0.71	53	0.62	42	1.63	28	0.98	1.5
C3	2110	1930	51.3	1.13	35	0.75	45	0.98	36	1.59	29	0.84	1.2
A0	2480	2040	39.6	0.95	42	0.88	46	0.81	41	1.54	40	0.66	1.4
A13	2730	2040	42.8	1.15	45	0.78	48	0.87	42	1.41	46	0.63	1.0
A14	3290	2020	35.2	1.35	50	1.11	49	1.01	50	1.63	51	0.52	1.0
A15	4070	2260	35.4	1.23	53	1.11	53	1.10	49	1.48	55	0.37	0.8
A16	5580	2400	34.3	1.17	60	1.20	59	1.15	62	1.19	59	0.01	0.6

Legend: D = downstream distance from confluence spit; W = width; H = median depth; U = median cross-sectional velocity magnitude; FD = median flow direction degrees from North; ΔU = difference between median velocity magnitudes of Negro and Solimões sections; $ΔU_{max}$ = maximum velocity magnitude difference; subscripts: N = Negro; MI = mixing interface; and S = Solimões portions of transect.

Through the central confluence region as the waters of the Negro and Solimões merge and realign with the downstream channel of the Amazon River the flow in all three portions of the confluence accelerates as confluence width narrows. Within this central confluence region a maximum depth-averaged velocity magnitude of approximately 2.5 m/s was observed near the right bank around transect C1. After the transect C1 the flow direction of the Solimões waters changes dramatically as it realigns with the flow direction of the Amazon River around transects A0 and A13. In Table 2, it can be seen that the median cross-sectional velocity magnitudes increase throughout the central confluence region until the transect C7 just before the beginning of the Amazon River. As the waters of the Negro and Solimões converge into the channel of the Amazon River, the cross-sectional averaged velocities decrease between transects C7 and A0/A13, which would seem to indicate the end of the flow acceleration generated by the reduction in confluence width through this central region. Between these transects, a flow separation and recirculation zone was observed just downstream of the junction corner of the Solimões and Amazon Rivers. Further in this region there seems to be a significant lateral deflection of the mixing interface as the flows realign with the Amazon channel, which may be related to the observed flow separation zone. Throughout, this central confluence region there was a substantial difference in velocity magnitude (i.e. ΔU up to 0.7 m/s) observed immediately about the mixing interface, these lateral differences in velocity magnitude occur over a relatively short distance (i.e. less than 70 m). Such a large difference and rapid change in velocity magnitudes about Solimões side of the mixing interface would seem to indicate that "velocity shear" was the primary mechanism driving the mixing in this region.

From transect A0 the median cross-sectional averaged velocities increase with distance downstream until reaching a maximum around the transect A14, after which the cross-sectional velocities decrease as the channel width expands. Under the flow conditions observed on 31/10/2014, complete realignment of the Negro and Solimões waters with the Amazon River channel occurred about the transect A13. Between transects A14 and A16 the median depth-averaged velocities of the Solimões portion decrease while those of the Negro and Mixing Interface portions increase. This would seem to indicate the transfer of momentum from the Solimões to the Negro side of the Amazon Channel.

2.1 Key hydrodynamic features observed during the Field Study CNS1

Figure 4 shows the approximate location of key hydrodynamic and morphodynamic features described in Section 1 about the confluence of the Negro and Solimões Rivers observed during the Field Study CNS1. In Figure 4, key hydrodynamic features are indicated by the numbers: (1) stagnation zone; (2) region of deflection; (3) downstream separation zone; (4) region of maximum velocity; (5) region of flow recovery; (6) mixing interface/shear layer; and (7) end of the confluence hydrodynamic zone. The approximate locations of the observed regions of deflection, maximum velocity on 31/10/2014 have been described in previous section. In Figure 4, the approximate location of the flow stagnation zone is highlighted in red, with the locations of the downstream flow separation zone and mixing interface highlighted in blue and green respectively. The approximate extents of the mixing interface are marked by a solid and dashed green lines, which indicate the boundaries between the Solimões/mixing interface and the mixing interface/Negro respectively.

The possible extent of the flow recovery region for the Field Study CNS1 are marked with dashed purple lines, with some evidence of a reduction in the confluences influence about transect A16 on 31/10/2014 (Table 2), thereby possibly indicating the beginning of the flow recovery region. Transects collected further downstream on 29/10/2014 indicate a gradual reduction in the velocity difference and asymmetric velocity profiles with distance downstream, with no velocity difference across cross-section at transect A7. The observation of near constant velocity distribution would seem to indicate the end of the confluence hydrodynamic zone about the transect A7, and therefore the finish of the flow recovery region for the low flow conditions observed during the Field Study CNS1. These two boundaries possibly indicate that the end of CHZ location changed with short-term variations in tributary flow conditions observed during the Field Study CNS1.

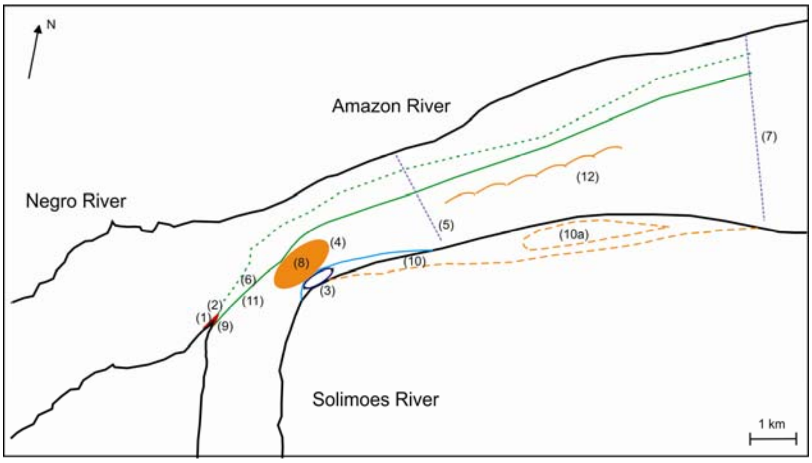

Figure 4. Map of key hydrodynamic features observed about confluence of Negro and Solimões Rivers during Field Study CNS1.

In Figure 4, the possible size and extent of the flow separation region and recirculation cell within the separation zone observed about the Solimões/Amazon junction corner during the Field Study CNS1 are shown in light and dark blue respectively. It is worth noting that on 31/10/2014, no separation region was easily discernable about the downstream junction corner of the Negro and Amazon Rivers. One possible explanation for this, could be the difference in the junction angles, with previous studies suggesting that the size of these downstream separation region increased with junction angle and are generally not present for junction angles less than 30° (e.g. Huang et al., 2002). The observed recirculation cell within the separation zone was located about transects C3, A0 and A13 and had a width of about 300 m and a length of approximately 1,000 m. As part of this recirculation cell, an upstream velocity magnitude of approximately 0.3 to 0.6 m/s was observed near the right bank at Sites A0 and A13. On 31/10/2014, the impact of the flow separation zone was still observed up to 250 m from the right bank at transect A15, but not clearly observable about transect A16 which would indicate that this separation zone had a length of over 2 km.

2.2 Hydrodynamics and mixing

For the flow condition observed during the Field Study CNS1 the position and size of the mixing interface is plotted in Figure 4. In Figure 4, it can be seen that the width of the mixing interface expands through the central confluence region between Sites C0 and C7. The physical width of the mixing interface seemed to reduce about the beginning of the Amazon River (e.g. from Site C7 to C3), however this corresponds to an increase in the width of the pure Solimões waters in this region (e.g. Figure 5), which could be related to the compression of the flows into the Amazon channel and the separation region on the Solimões/Amazon junction corner deflecting the Solimões waters towards the centre of the channel. Figure 5 shows the percentage of the transect width occupied by the pure waters of the Negro and Solimões Rivers as well as the mixing interface as functions of distance downstream from the confluence junction spit. In Figure 5, it can be seen that on 31/10/2014 the percentage of the channel width occupied by pure Solimões waters gradually increases over the study region between Sites C0 and A16. At the beginning of the Amazon River, after Site A0 the percentage of width occupied by the mixing interface and pure Negro waters seemed to decrease at a relatively similar rate, both being approximately 16 % of channel width by Site A16. The change in the width occupied by pure Negro waters over the study region on 31/10/2014 is equivalent to an approximately 80 % reduction in the cross-sectional area occupied by pure Negro waters between the end of Negro River at Site N-CNS and Site A16 located approximately 5.5. km downstream. This represents a significant reduction in the discharge ratio between the Negro and Solimões waters ($Q_R = Q_N/Q_S$), that is from 0.38 at the beginning of the CHZ to approximately 0.15 at Site A16, which is just 2 post-confluence channel widths downstream from the beginning of confluence. This would seem to indicate a relatively high rate of mixing occurred within the CHZ during the Field Study CNS1, and further the observed rate of mixing seemed greater than that observed in studies such as Laraque et al. (2009) at the same confluence under similar flow conditions.

During CNS1 the primary mixing mechanism within the central CHZ region was most likely velocity shear about the interface of these waters, with the maximum lateral rate of change in velocity magnitude $(dU/dy)_{max}$ being approximately 0.02 (m/s)/m on the Solimões side of the mixing interface at Sites C0 through to A0. Within the downstream CHZ between Sites A13 and A16 $(dU/dy)_{max}$ was about 0.004 (m/s)/m which could conceivably indicate the reduced impact of velocity shear within this region. Visual observations by the lead author of the waters about the confluence of the Negro and Solimões Rivers during the Field Study CNS1 found evidence of several different types of flow structures and possible mixing mechanisms within and immediately about the mixing interface which have been sited in previous experimental confluence studies, these include for example:

- Kelvin-Helmholtz and asymmetric (e.g. Holmboe) instability waves about the stratified mixing interface;
- Lateral rolling over of these instability waves, forming large vortices of Solimões waters with diameters of up to 40 m;
- Lateral bursting of these large vortices relative large distances (i.e. 100's m) into Negro side of mixing interface;
- Some slight overturning/inclination of stratified layer within mixing interface (i.e. Negro over Solimões waters) further downstream, however initial analysis of ADCP data indicates this overturning was intermittent;
- In central CHZ regions large turbulent surface boils (> 50 m) on Solimões side of mixing interface with no boils observed on Negro side or in mixing interface, indicating impact of stratified mixing interface on local hydrodynamics;
- Further downstream, large turbulent boils were observed on Negro side and within the mixing interface as well as on Solimões side of channel.

Unfortunately it was not possible to collect stationary ADCP measurements during the Field Study CNS1 and therefore it is not possible to study in detail the observed flow structures and mixing mechanisms observed about the mixing interface generated about the confluence of the Negro and Solimões Rivers.

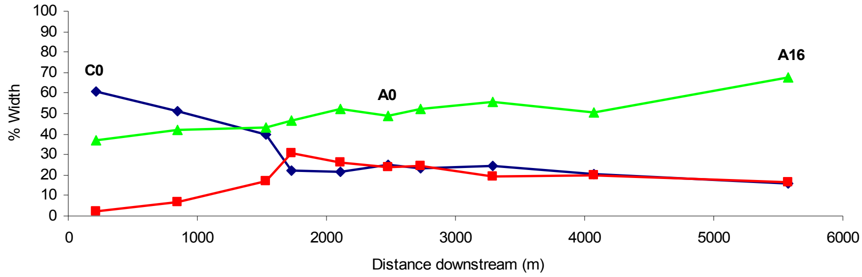

Figure 5. Percentage of transect width of individual sections (i.e. Negro, Solimões and Mixing interface waters) as a function of distance downstream of confluence. Legend: — pure Negro waters; — pure Solimões waters; — mixed waters (i.e. mixing interface).

2.3 Hydrodynamics and sediment transport/morphodynamics

Figure 4 also highlights several common morphodynamics features were also observed during the Field Study CNS1, these included: (8) scour hole; (9) deposition about stagnation zone; (10) deposition about downstream separation zone; and (11) deposition bars about centre of channel; as well as (12) large bed forms on the Solimões side of the Amazon channel. In Figure 4, these morphodynamic features are highlighted in orange when possible, for example the potential site of the scour hole. It should be noted that scale and location for some of the observed morphodynamic features such as deposition about the stagnation and separation zones as well as bars in central channel would seem to indicate that these features formed under past high flow conditions than in the observed low flow conditions during Field Study CNS1.

Figure 6A shows the longitudinal profile LS from WinRiver 2 collected along the Solimões side of confluence on 01/11/2014 as part of the Field Study CNS1. In Figure 6A a scour hole (between 1,000 and 2,500 m) is observed about the region of highest flow velocities and has the dimensions of approximately 1.5 km long, 700 m wide and 20 m deep (e.g. Figure 4). Also in Figure 6A, a region of relatively large bed-forms located downstream of transect A16 were observed during the Field Study CNS1. These bed-forms change in shape and height throughout this region with heights and wavelengths up to 10 and 200 m respectively. It is worth noting that no bed-forms were observed on the Negro side of the channel. At several transects within the central CHZ region there is some evidence of relatively large bars (e.g. at C0 bar with approximate height = 5 m and width = 150 m) formed about the mixing interface (e.g. Figure 6B). In such transects where these bar features were observed, a downward velocity is typically observed at the Solimões side of the mixing interface, which would seem to indicate deposition of sediments allowing the formation of these structures. Further, seismic profiles within the central CHZ seem to indicate no sediment deposition on the Negro side of the mixing interface, which conceivably indicates that the stratified shear layer inhibits the transfer of sediment across the mixing interface in this region. Figure 6B shows the cross-sectional profile of backscatter intensity collected at Site C0 on 31/10/2014. In Figure 6B, it can be seen that this bar feature restricts the local depth of interaction between the Negro and Solimões waters to approximately 6 m, with some local bed discordance between the Solimões and Negro channels observed. Throughout the study region the level and type of local bed concordance ($H_N > H_S$; $H_N = H_S$; $H_N < H_S$) varied significantly from site to site. Finally some evidence of deposition about the stagnation (e.g. central shallow region about Site C0, i.e. 2,500 to 3,500 m in Figure 6B) and downstream separation zones were also observed in the ADCP and seismic transects with these areas of deposition usually associated with low and/or re-circulating flow velocities near the banks. Within these depositions regions finer sediments were observed in the seismic profiles and from visual observations about the bank about central and Solimões/Amazon junctions.

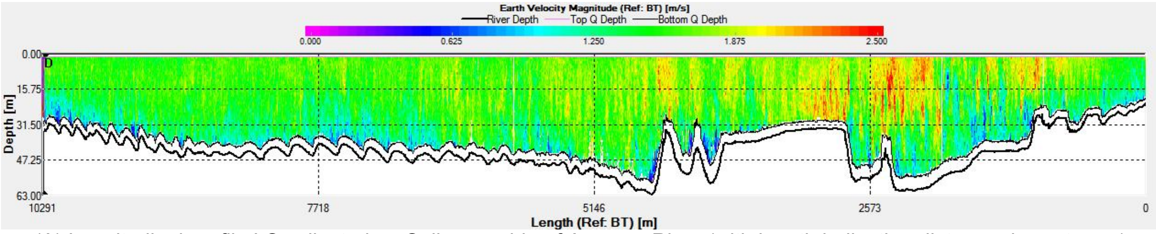

(A) Longitudinal profile LS collected on Solimões side of Amazon River (with length indicating distance downstream)

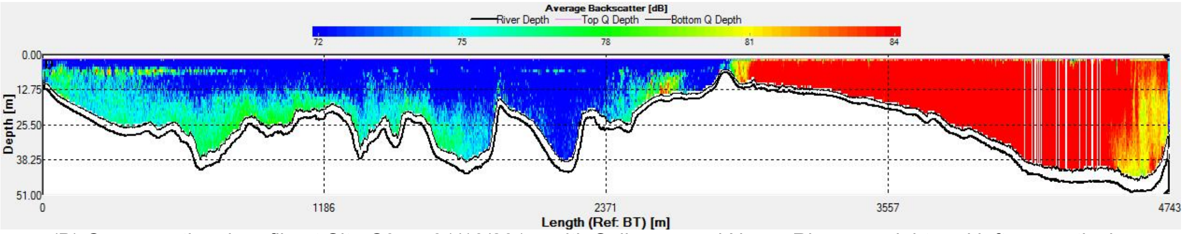

(B) Cross-sectional profile at Site C0 on 31/10/2015, with Solimões and Negro Rivers on right and left respectively.

Figure 6. ADCP transects from WinRiver 2 illustrating key morphological features observed about confluence during Field Study CNS1.

2.4 Comparison with past data collected under extreme low and high flow conditions

Between 2009 and 2013 the CPRM (Geological Survey of Brasil) collected some ADCP transects at several locations about the confluence hydrodynamic zone of the Negro and Solimões Rivers. This section compares two of these transects collected at Sites C2 and C3 under extreme low (Q_S = 36,200 m^3/s) and high (Q_S = 152,400 m^3/s) flow conditions on the Solimões River on 20/09/2010 and 13/07/2013 with transects collected about the same locations during the Field Study CNS1 (Q_S = 75,500 m^3/s). Table 3 presents the measured flow conditions, observed median cross-sectional flow properties and width of the mixing interface at each sampling site. Site C2 is situated within the central confluence region approximately 1.4 km from the point of the central junction spit as observed during the Field Study CNS1, while Site C3 is located about the beginning of the Amazon River channel approximately 2 km downstream of the central junction spit. The channel widths at Sites C2 and C3 during the Field Study CNS1 were approximately 2.7 and 2.0 km respectively, with median cross-sectional depths of 40 and 50 m.

Table 3. Flow characteristics of ADCP transects collected by CPRM about confluence of Negro and Solimões Rivers 2009 to 2013 .

	Q_S (MAN) (m^3/s)	Q_N (PAR) (m^3/s)	Q_R	SITE	W_{MI} (m)	U_N (m/s)	FD_N (°)	U_{MI} (m/s)	FD_{MI} (°)	U_S (m/s)	FD_S (°)	ΔU (m/s)	$ΔU_{max}$ (m/s)
20/10/2010	36,200	35,500	1.0	C2	61	0.63	61	0.57	43	0.96	59	0.33	0.7
30/10/2014	75,500	24,500	0.3	C2	316	0.48	60	0.42	43	1.58	48	1.10	1.7
13/07/2013	152,400	56,500	0.4	C3	42	1.27	49	1.18	45	2.07	31	0.80	2.0
31/10/2014	75,500	24,000	0.3	C3	501	0.75	45	0.88	39	1.50	30	0.75	1.2

Legend: Q_S (MAN) = Solimões River discharge at Manacapuru station; Q_N (PAR) = Negro River discharge at Paricatuba station; Q_R=Q_N/Q_S discharge ratio of Negro and Solimões Rivers; W_{MI} = width of mixing interface; U = median cross-sectional velocity magnitude; FD = median flow direction degrees from North; ΔU = difference between median velocity magnitudes; $ΔU_{max}$ = maximum velocity magnitude difference; subscripts: N = Negro; MI = mixing interface; and S = Solimões portions of transect.

At both Sites C2 and C3, one of the clearest distinctions observed from the ADCP transects collected during Field Study CNS1 and those collected under extreme low and high Solimões flow conditions is the width of mixing interface. In Table 3, it can be seen that the mixing interface widths during the extreme high (13/07/2013) and low (20/10/2010) flow conditions are significantly narrower than those observed about the same location during the Field Study CNS1, as shown in the depth-averaged backscatter intensity data presented in Figure 7. Figure 7 presents the depth-averaged velocities and backscatter intensity (BS) as a function of distance over the transect length for the transects presented in Table 3. In Figures 7A and 7C, a rapid change in the depth-averaged backscatter intensity can be observed about the mixing interface under both extreme low and high flow conditions, while during Field Study CNS1 (Figures 7B and 7D) a more gradual change in backscatter intensity is observed about the mixing interface. As mentioned in Section 2.1, a relatively high rate of mixing about and downstream of the Negro/Solimões confluence was observed during the Field Study CNS1. Therefore the significantly smaller mixing interface width observed about Sites C2 and C3 on 20/09/2010 and 13/07/2013 would seem to indicate that only limited mixing occurred under both the extreme low and high flow conditions observed on these dates. Further a comparison of the mixing interface widths on 20/09/2019 and 13/07/2013 would seem to indicate that less mixing occurred under extreme high flow conditions than extreme low flow conditions.

Figure 7 also shows the variation in depth-averaged East, North and Vertical velocities over the transects at C2 (Figures 7A and 7B) and C3 (Figures 7C and 7D) on the dates presented in Table 3. In Figure 7, under all flow conditions a significant difference between the depth-averaged North and East velocities can be observed on the Solimões (right) side of the cross-section with dominance of the North velocities increasing towards the Southern bank of the confluence. Conversely, the magnitude of the depth-averaged North and East velocities are relatively similar on the Negro side of the mixing interface. This would seem to be related to the relative channel alignments of the Negro and Solimões Rivers in relation to that at the beginning of the Amazon River, with the observations during the Field Study CNS1 indicating that this difference between North and East velocities was smaller at Site C3 than at Site C2.

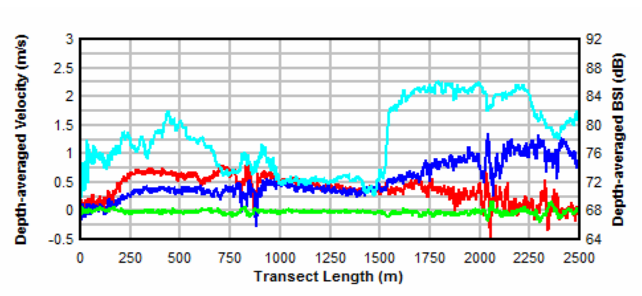

(A) Site C2 on 20/09/2010

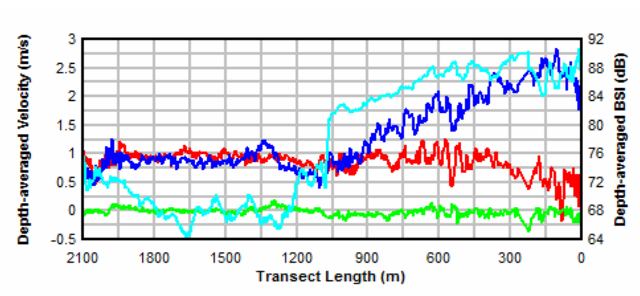

(C) Site C3 on 13/07/2013

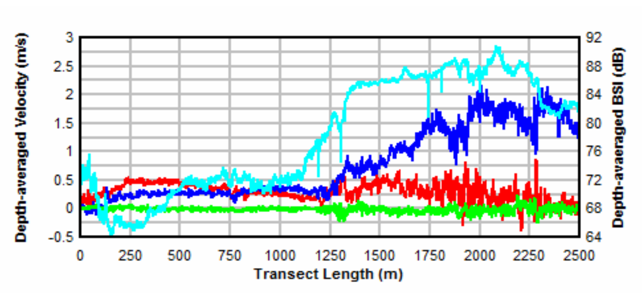

(B) Site C2 on 30/10/2014

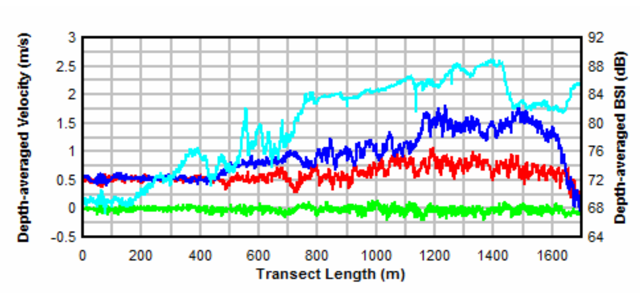

(D) Site C3 on 31/10/2014

Figure 7. Comparison of depth-averaged velocities and backscatter intensity (BS) about Sites C2 an C3 under extreme low (20/09/2010) and high (13/07/2013) flow conditions with those observed during Field Study CNS1 (28-31/10/2014). Legend: —— East velocity; —— North velocity; —— Vertical velocity; —— Backscatter intensity.

3. DISCUSSION

Of the thousands of natural confluences on Earth, only detailed studies of around one hundred confluences have been presented in peer review publications, with most of these studies concentrating on confluence morphodynamic (e.g. Rhoads et al., 2009) and mixing (e.g. Lane et al., 2008) processes. Conversely, the majority of our present understanding on confluence hydrodynamics has been developed from laboratory flume experiments (e.g. Best, 1987; Gurram et al., 1997), with an extremely limited number of detailed hydrodynamic measurements being conducted in natural confluences. To date, the vast majority of these studies have been conducted in small confluences (e.g. Rhoads and Kentworthy, 1998), although more recently some detailed hydrodynamic studies have been conducted in relatively large confluences (e.g. Konsoer and Rhoads, 2014). The hydrodynamic data presented herein, which was collected about the confluence of the Negro and Solimões Rivers during the Field Study CNS1 is representative of the largest confluence hydrodynamics study to date, with this confluence being approximately an order of magnitude larger than those presently published. Therefore, despite the early stages of this investigation, it is worthwhile to conduct a brief initial comparison of the observed hydrodynamics from this large confluence study, with those collected in past laboratory and smaller natural confluence studies, and highlight some topics that require future investigation.

During the Field Study CNS1, all key hydrodynamic features of confluences (e.g. Figure 1) outlined in past studies such as Best (1987) were observed about the confluence of the Negro and Solimões Rivers (e.g. Figure 4). Further the flow patterns of depth-averaged velocity profiles observed about the Negro/Solimões confluence on 31/10/2014 (Figure 3) are very similar to those presented in Figure 4 from the flume study by Gurram et al. (1997) for $\alpha = 90°$ and $q = 0.75$. This would seem to indicate that large scale hydrodynamics (e.g. depth-averaged velocity patterns) scale reasonably well with large variations in confluence size. However one noticeable region of difference between flume and natural confluences dynamics seems to be within the downstream region of the CHZ where the magnitude of velocity difference across the mixing interface, the length of flow recovery and mixing length seem to differ, with these generally seeming smaller in flume studies (e.g. Huang et al., 2002). Another example of this possible discrepancy relates to the separation zone about the Solimões/Amazon junction corner observed during the Field Study CNS1. Such downstream separation regions have rarely been reported during past field experiments in smaller natural confluences (e.g. Rhoads and Kentworthy, 1998). For the observed discharge ratio (q = QS/QA ≈ 0.7) and junction angle (α = 80°) for the Negro/Solimões confluence, the theoretical models presented in previous studies (e.g. Best and Reid, 1984; Gurram et al.,1997) seem to over estimate the relative length and width of the observed separation zone about the Solimões/Amazon junction by a factor of two. The reasons for these discrepancies between the predicted and actual separation region size is presently unclear at this early stage of the investigation.

One possible explanation for these differences in observed flow properties within the downstream CHZ region between flume and natural confluence studies could be the difference in water characteristics of incoming flows observed in all natural confluences (e.g. Rhoads and Kentworthy,1998; Konsoer and Rhoads, 2014), while the water characteristics in flume studies are generally identical (e.g. Best, 1987). In the vast majority of previous studies about natural confluences some difference in water characteristics between the incoming flows was observed, whether this be in terms of temperature (e.g. Rhoads and Sukhodolov, 2008), suspended sediment concentration (e.g. Lane et al., 2008) or both (e.g. Konsoer and Rhoads, 2014). Previous studies such as Ramon et al. (2013) have shown that the difference in water characteristics may also vary with local season changes within the tributary catchments, which cause local changes in the relative water densities between the two incoming waters at the confluence. The impact of these water characteristic differences seems to increase with the relative size of the confluence, with previous studies relating this increased effect to the relative size and spatial distribution of the tributary catchments (e.g. Lane et al., 2008; Ramon et al., 2013). That is, as the size and spatial distribution of the catchments increase so to does the likelihood of greater variations in water characteristics between the incoming flows, and conceivably more importantly as the size of the confluences increases so to do the forces acting on the merging waters generated by the increased discharge (e.g. Table 4). Table 4 shows the flow properties of a small (Rhoads and Sukhodolov, 2008), a large (Konsoer and Rhoads, 2014) and very large (present study, 2015) confluences to demonstrate the change in forces (e.g. momentum flux) with tributary discharge. In Table 4, it can be seen that the confluence forces such as tributary momentum flux increase proportionally with discharge and are significantly greater about large confluences.

Table 4. Flow properties for a small, large and very large confluence.

	Tributary	Q (m^3/s)	U (m/s)	W (m)	H (m)	M (kgm/s^2)
PRESENT STUDY (2015)	SOLIMÕES RIVER	63,380	1.34	1,700	25.0	85,717,573
	NEGRO RIVER	24,030	0.4	2,700	25.2	9,591,000
KONSOER AND RHOADS (2014)	WABASH RIVER	1,351	0.97	221	6.3	1,311,730
	WHITE RIVER	1,220	1.04	171	6.9	1,266,320
RHOADS AND SUKHODOLOV (2008)	COPPER SLOUGH	0.75	0.45	8.5	0.19	337
	KASKASKIA RIVER	0.35	0.19	6.8	0.28	65

Legend: Q = discharge; U = cross-sectional velocity magnitude; W = width; H = depth; M = momentum flux

The force created by the tributary momentum flux has both a lateral and streamwise component relative to the downstream channel, since both tributaries enter the confluence at unique angles, with the relative magnitude of the lateral component increasing with the relative angle between the tributary and downstream channel. This lateral component of the momentum flux is important in confluences because it acts towards the mixing interface creating a pressure which pushes the two waters together (e.g. Figure 12 from Huang et al., 2002). Huang et al. (2002) showed that the distance between streamlines decreased about the mixing interface as the junction angle was increased, which also indicated that the lateral pressure acting the mixing interface increased. In natural confluences where the tributary waters have different water characteristics, these lateral pressure forces push the two different waters together and thereby the corresponding density differences occur over a relative short distance (e.g. Figures 7A and 7C). If this lateral pressure acting on the mixing interface is great enough then this interface will become laterally stratified, which in turn can have a significant impact on the local hydrodynamic and mixing processes about the mixing interface (e.g. Rhoads and Kentworthy, 1998). In fluid mechanics, the Richardson number (e.g. gradient Richardson number $R_{lg} = (g'/dz)/(dU/dz)^2$, where dU = velocity difference; dz = distance of change; and $g' = g\Delta\rho/\rho_0$) has been extensively used to determine the level of stratification about the interface of two different density fluids and the impact this stratification has on the local flow properties about the mixing interface (e.g. Strang and Fernando, 2001). Flume studies about vertical stratification such as that of Strang and Fernando (2001) have used the Richardson number to explain the mixing mechanisms and flow structures (e.g. Kelvin-Helmholtz waves) observed about the mixing interface, all of which have been noted by previous studies about the mixing in natural confluences (e.g. Rhoads and Sukhodolov, 2008). Bridge (1993) suggested that the flow structures and mixing mechanisms (e.g. Kelvin-Helmholtz instabilities) observed about the mixing interface in natural confluences was dependent on the Reynolds and Richardson numbers. However to date no previous studies in natural confluences has utilised the Richardson number to explain the impact of this difference in water characteristics and thereby water densities between the two incoming flows. A separate study by the lead author into the use and validity of applying the Richardson number to lateral stratification about the mixing interface is presently underway.

The initial analysis presented herein seems to indicate that relative large velocity shear about the mixing interface was the primary mechanism driving the relatively rapid mixing observed about the Negro/Solimões confluence on 31/10/2014 (Field Study CNS1). However as mentioned in Section 2.1 some slight overturning of the mixing interface may have been observed intermittently within downstream CHZ region during the Field Study CNS1. The review of Biron and Lane (2008) indicted that overturning is quite common in larger confluences and seemed to be the primary mechanism behind the relatively rapid mixing cases observed about the Paraguay/Parana confluence in Lane et al. (2008) and the Negro/Solimões confluence in 1997 reported in several studies (e.g. Laraque et al., 2009; Maurice-Bourgoin et al., 2003). In Lane et al. (2008), complete overturning was observed which led to complete mixing being observed 8 km downstream (i.e. Mixing length < 4 $W_{Dowstream}$). While Maurice-Bourgoin et al. (2003) reported that a mass balance indicated that complete mixing of the Negro and Solimões waters seemed to occur 25 km downstream (i.e. Mixing length ≈ 10 $W_{Dowstream}$). However ADCP surface water temperature data presented in Figure 4 of Laraque et al. (2009) showed some stratification at 25 km and would seem to indicate that complete mixing did not seem to occur until approximately 100 km downstream. An initial comparison between this 1997 study and the present study (CNS1) would seem to indicate that the rate of mixing observed downstream of Negro/Solimões confluence for CNS1 was conceivably more rapid than under similar low flow conditions in 1997 (e.g. Laraque et al., 2009).

More recently Ramon et al. (2013) proposed a concept model using of the internal Froude number ($F_i = U/(g'h)^{1/2}$, where U = inflow velocity; h = channel depth; and $g' = g\Delta\rho/\rho_0$) and the inflow velocity ratio (U_R) to determine the behaviour of the mixing interface in natural confluences and whether overturning will occur. In fluid mechanics, the internal Froude number is used to determine whether the inertial or buoyancy forces will dominate about a stratified shear layer, mainly about vertical stratification layers. Ramon et al. (2013) based on field sampling conducted about the relatively large confluence of the Ebro and Segra Rivers indicated that for: $F_i >> 1$ inertia dominates, the effect of density differences become negligible and the mixing interface orientation remains relatively vertical; $F_i < 1$ vertical stratification begins to form through overturning; $F_i << 1$ buoyancy dominates causing complete overturning (e.g. Lane et al., 2008), and $F_i > 1$ weekly buoyant side flows with mixing interface significantly distorted further citing as an example the Negro/Solimões confluence (e.g. Laraque et al., 2009). Finally visual observations by the lead author about the confluence indicate that long-period velocity oscillations in the tributary flows especially the Solimões River may have a significant effect on the local flow structures and mixing mechanisms about the mixing interface. For example, velocity fluctuations about the mean flow velocity by long-period oscillations and large macro-turbulence seemed to cause the lateral roll over of the mixing interface instability waves (e.g. Kelvin-Helmholtz) creating large vortices of Solimões waters and subsequent lateral bursting of these vortices 100's of metres towards Negro side. Further, previous studies such as Barua and Rahman (1998) and Parsons et al., (2007) have shown that the interaction of the flow with upstream topographical and local bathymetrical features in rivers can have a significant impact on the local flow properties (Section 1). Therefore it is important to study the influence of long-period oscillations and the interaction of the flow with the local bathymetry to better understand the hydrodynamics about large confluences.

4. CONCLUSIONS

Presented herein are some initial observations from ADCP transects and water samples collected about the confluence of Negro and Solimões River in October 2014, which include: differences in tributary water characteristics created lateral stratification about mixing interface; a rapid lateral change in velocity about mixing interface seemed to indicate that velocity shear had significant role in mixing processes; relatively rapid mixing of the Negro and Solimões waters within the CHZ, and observation of common hydrodynamic and morphodynamic features noted in previous confluence studies. Further, a comparison with past data collected about the Negro/Solimões confluence seemed to indicate that the observed mixing was significantly more rapid than that observed under extreme high and low flow conditions, indicating these could represent relative slow mixing events. To date, this is the largest confluence in which detailed hydrodynamic measurements have been undertaken and a brief initial comparison to previous studies collected in smaller natural and laboratory confluences seemed to indicate: some differences in the observed flow properties and structures within the initial portion of the downstream channel between laboratory and natural confluences, these differences could be related to the difference in tributary water characteristics observed in natural confluences; the significance of the difference in water characteristics seems to increase with size of confluence through greater forces generated by the larger flows. From the initial findings presented herein, this study hopes to investigate the effect on the local hydrodynamics in confluences from: lateral stratification about mixing interface; long-period oscillations in flow velocity; local confluence bathymetrical features; and variations basin scale processes.

ACKNOWLEDGMENTS

The authors acknowledge this research was carried out within the CLIM-AMAZON European Laboratory in Brazil funded by grant agreement FP7 INCO-LAB n° 295091 from the European Commission; the CPRM (Geological Survey of Brasil) and Prof. Roberto Ventura Santos for supplying the research vessel, instrumentation, technical assistance with sampling and ADCP transects collected about confluence between 2009-2013; and finally Bosco Alfenas, Daniel Moreira, Paulo Melo, Nilda Pantoja and Joao Andrade for their assistance with sampling during the field campaign.

REFERENCES

Barua, D., and Rahman, K. (1998). Some aspects of turbulent flow structure in large alluvial rivers. *Journal of Hydraulic Research*, 36(2), 235-252.

Best, J. (1987). *Flow* dynamics at river channel confluences: implications for sediment transport and bed morphology. *Recent Developments in Fluvial Sedimentology*, (Eds. Ethridge, F., Flores, M. and Harvey, M.,), Spec. Publ. 39, Society of Economic Paleontologists and Mineralogists, 27-35.

Best, J. (1988). Sediment transport and bed morphology at river channel confluences. *Sedimentology*, 35, 481-498.

Best, J.L., and Rhoads, B.L. (2008). Sediment transport, bed morphology and the sedimentology of river channel confluences. *River confluences, tributaries and the fluvial network*, (Eds: Rice, S., Roy, A. and Rhoads, B.), J.Wiley & Sons, 45-72.

Best, J. and Reid, I. (1984). Separation zone at channel junctions. *Journal of Hydraulic Engineering*, 110, 1588-1594.

Biron, P., and Lane, S. (2008). Modelling hydraulics and sediment transport at river confluences. *River confluences, tributaries and the fluvial network*, (Eds: Rice, S., Roy, A. and Rhoads, B.), J.Wiley & Sons, 17-43.

Bridge, J. (1993). The interaction between channel geometry, water flow, sediment transport and deposition in braided river. *Braided Rivers* (Eds. Best, J. and Bristow, C.), Geological Society Special Publication No. 75, 13-71

Constantinescu, G., Miyawaki, S., Rhoads, B., Sukhodolov, A., and Kirkil, G. (2011) Structure of turbulent flow at a river confluence with a momentum and velocity ratios close to 1: insight from an eddy-resolving numerical simulation. *Water Resources Research*, 47, W05507, 16 pages

Kentworthy, S. and Rhoads, B. (1995). *Hydrologic* control of spatial patterns of suspended sediment concentration at a stream confluence. *Journal of Hydrology*, 168, 251-263.

Konsoer, K., and Rhoads, B. (2014). Spatial–temporal structure of mixing interface turbulence at two large river confluences. *Environmental Fluid Mechanics*, 14(5), 1043–1070.

Gurram, S., Karki, K. and Hager, W. (1997). Subcritical junction flow. *Journal of Hydraulic Engineering*, 123(5), 447-455.

Gaudet, J. and Roy, A. (1995). Effect of bed morphology on flow mixing length at river confluences. *Nature*, 373, 138-139.

Huang, J., Weber, L. and Lai, Y. (2002). Three-dimensional numerical study of flows in open-channel junctions. *Journal of Hydraulic Engineering*, 128(3), 268-280.

Lane, S., Parsons, D., Best, J., Orfeo, O., Kostaschunk, R. and Hardy, R. (2008). Causes of rapid mixing at a junction of two large rivers: Rio Parana and Rio Paraguay, Argentina. *Journal of Geophysical Research*, 113, F02019, 16 pages.

Laraque, A., Guyot, J., and Filizola, N. (2009). Mixing processes in the Amazon River at the confluences of the Negro and Solimões Rivers, Encontro das Aguas, Brazil. *Hydrological Processes*, 23, 3131-3140.

MacKay, J. (1976). *Lateral* mixing of the Laird and Mackenzie rivers downstream from their confluence. *Canadian Journal of Earth Sciences*, 7, 111-124.

Maurice-Bourgoin, L., Quemerais, B., Moreira-Turcq, P. and Seylar, P. (2003). Transport, distribution and speciation of Mercury in the Amazon River at the confluence of black and white waters of the Negro and Solimões Rivers. *Hydrological Processes*, 17, 1405-1417.

Mosley, P. (1976). An Experimental study of channel confluences. *Journal of Geology*, 84, 535-562.

Parsons, D., Best, J., Lane, S., Orfeo, O., Hardy, R. and Kostaschuk, R. (2007). Form roughness and the absence of secondary flow in a large confluence-diffluence, Rio Parana, Argentina. *Earth Surface Processes and Landforms*, 32, 155-162.

Parsons, D., Best, J., Lane, S., Kostaschuk, R., Hardy, R., Orfeo, O., Amsler, M. and Szupiany, R. (2008). Large river channel confluences. River Confluences, *Tributaries and the Fluvial Network* (Eds: Rice, S., Roy, A. and Rhoads, B.), J.Wiley & Sons, Ltd, 73-91.

Parsons, D., Jackson, P., Czuba, J., Engel, F., Rhoads, B., Oberg, K., Best, J., Mueller, D., Johnson, K. and Riley, J. (2013). Velocity Mapping Tool (VMT): a processing and visualization suite for moving-vessel ADCP measurements. *Earth Surface Processes and landforms*, 38, 1244-1260.

Ramon, C., Hoyer, A., Armengol, J., Dolz, J. and Rueda, F. (2013). Mixing and circulation at the confluence of two rivers entering a meandering reservoir. *Water Resources Research*, 49, 1429-1445.

Rhoads, B. and Kentworthy, S. (1998). Time-averaged flow structure in the central region of a stream confluence. *Earth Surface Processes and Landforms*, 23, 171-191.

Rhoads, B. and Sukhodolov, A. (2008). Lateral momentum flux and the spatial evolution of flow within a confluence mixing interface. Water *Resources Research*, 22, W08440, 17 pages.

Rhoads, B., Riley, J. and Mayer, D. (2009). Response of bed morphology and bed material texture to hydrological conditions at an asymmetrical confluence. *Geomorphology*, 109, 161-173

Richey, J., Meade, R., Salati, E., Devol, A., Nordin, C. and Santos, U. (1986). Water discharge and suspended sediment concentration in the Amazon River: 1982-1984. *Water Resources Research*, 22(5), 756-764.

Strang, E. and Fernando, H. (2001). Entrainment and mixing in stratified shear flows. *Journal of Fluid Mechanics*, 428, 349-386.

Szupiany, R., Amsler, M., Parsons, D. and Best, J. (2009). Morphology, flow structure and suspended bed sediment transport at large braid-bar confluences. *Water Resources Research*, 45, W05415, 19 pages.